Degradable Hyaluronic Acid/Chitosan Polyelectrolyte Multilayers with Marine Fouling-Release Properties

Wenfa Yu†, Robin Wanka†, John A. Finlay‡, Jessica L. Clarke‡, Anthony S. Clare‡, Axel Rosenhahn†*

† Analytical Chemistry- Biointerfaces, Ruhr University Bochum, Universitaetsstrasse 150, Bochum, 44801, Germany

‡ School of Natural and Environmental Sciences, Newcastle University, Newcastle upon Tyne NE1 7RU, United Kingdom

* Corresponding Author:

Axel Rosenhahn:

axel.rosenhahn@rub.de

Abstract: Polysaccharide multilayers consisting of hyaluronic acid and chitosan were prepared by layer-by-layer assembly. To be used in seawater, the multilayers were crosslinked to a different degree using thermal or chemical methods. ATR-FTIR revealed different amide densities as result of the crosslinking conditions. AFM showed that crosslinking affected the roughness and swelling behavior of the coatings. Stability and degradability of the multilayers in aqueous environments was monitored with spectroscopic ellipsometry. Resistance of the coatings against non-specific protein adsorption was characterized by SPR spectroscopy. Settlement assays using *Ulva linza* zoospores and removal assays using the diatom *Navicula incerta* showed that the slowly degradable coatings were less prone to fouling than the strongly crosslinked ones. Thus, the coatings were a suitable model system to show that crosslinking the multilayers under mild condition and equipping the coatings with controlled degradation rates enhances their antifouling and fouling-release properties against marine fouling organisms.

Keywords: Hyaluronic acid, chitosan, layer-by-layer, marine antifouling, fouling-release coatings, self-polishing coatings.

Introduction

Marine biofouling, a worldwide problem in maritime industries (Townsin 2003; Schultz et al. 2011) leads to massive ecological and economic costs. For instance, it is estimated that for a midsized naval ship, biofouling causes a financial loss in the order of 56 Million US Dollar per year (Schultz et al. 2011). This problem is usually counteracted by the use of antifouling paints which release toxic compounds into the sea. With recently growing ecological concerns, more effort is being devoted to the development of alternative environmentally benign coatings. Among the most promising current products are fouling-release coatings which use the shear force created by the water when a vessel moves through the ocean in order to self-clean. Such coatings are capable of reducing the attachment strength of marine organisms, allowing easy removal of fouling organisms in a sustainable way without the need for biocides (Lejars et al. 2012; Leonardi and Ober 2019). Coating properties such as topography (Cao et al. 2010), surface energy (Schilp et al. 2007), hydration (Rosenhahn et al. 2008), elastic modulus (Hu et al. 2009), and charge (Rosenhahn et al. 2009) have an effect on the interactions between the surface and marine microorganisms. Researchers have developed antifouling coatings with specific properties of surface energy (Brady and Singer 2000; Petrone et al. 2011; Rosenhahn and Sendra 2012), nanotopographies (Efimenko et al. 2009) and surface chemistries with high hydration and wettability (Kim et al. 2015; Wanka et al. 2018). These properties control settlement preferences and the adhesion strength of microorganisms.

Layer-by-layer (LbL) assembled polyelectrolyte multilayer (PEMs) is a thin film deposition technique introduced by G. Decher in the 90s (Decher 1997), has been widely adopted in multiple disciplines (Lichter et al. 2009; Moskowitz et al. 2010; Zhou et al. 2010) including preparing low-fouling coatings (Cao et al. 2010; Zhu et al. 2013; Zhu et al. 2015; Xu et al. 2016; Yu et al. 2019). The construction of PEMs is driven by various interaction forces among which electrostatic interactions are frequently exploited (Arys et al. 2001). Polysaccharides are naturally occurring biomacromolecules, display biocompatibility and biodegradability, and they are accessible in sufficient quantities. Thus, they are used in various applications such as food industry (Arnon et al. 2015) and biomaterials (Keskin et al. 2005; Zhou et al. 2010). The polysaccharides are highly hydrophilic and hydrated because of their functional groups such as hydroxyls, carboxylates, and amines. The hydrophilicity and high hydration of the polysaccharides is correlated with their resistance against protein adsorption (Liu et al. 2014), bacteria adhesion, and cell adhesion (Morra and Cassineli 1999). Polysaccharides have also been used as marine antifouling materials in several studies where they showed good antifouling performance against zoospores of the macroalgae *Ulva linza* (Cao et al. 2009; Bauer et al. 2013; Jakobi et al. 2018), the marine bacterium *Cobetia marina* (Bauer et al. 2013), the diatoms *Navicula incerta* (Bauer et al. 2013) and *Navicula perminuta* (Jakobi et al. 2018), and the cyprids of the barnacle *Balanus amphitrite* (Cao et al. 2009). Chitosan (Ch) (Figure. 1a) is a polysaccharide composed of N-acetyl-β-D-glucosamine and β-D-glucosamine linked (1→4) (Kujawa et al. 2005) and known for its antimicrobial activity (Tsai and Su 1999; Kong et al. 2010). In conjunction with ZnO, nanoparticle hybrid coatings were developed with excellent antifouling properties against pathogenic bacteria and several marine fouling species (Dhillon et al. 2014; Al-Naamani et al. 2017; Kumar et al. 2019). The potential of Ch to inhibit organism's attachment has been evaluated against freshwater bacteria (Fujimoto et al. 2006; Sanpui et al. 2008; Xing et al. 2009) and against marine species (Reda et al. 2017). Hyaluronic acid (HA) (Figure. 1b), consisting of alternating N-acetyl-β-D-glucosamine and β-D-glucuronic acid residues linked (1→3) and (1→4) respectively (Kujawa et al. 2005), is a naturally

occurring anionic polysaccharide present in the extracellular matrix of living organisms. HA shows high resistance against accumulation of cells, protein, and bacteria (Morra and Cassineli 1999; Pitt et al. 2004), which is attributed to its high hydration, and it has also been investigated as marine antifouling material (Cao et al. 2009; Bauer et al. 2013). Since both HA and Ch carry charges, they can be easily constructed into PEMs via LbL assembly. In fact, HA/Ch multilayers are intensively investigated as fouling-resistant coatings against freshwater bacteria (Richert et al. 2004; Del Hoyo-Gallego et al. 2016; Muzzio et al. 2017) and against protein adsorption (Croll et al. 2006). However, most of the applications are based on low ionic strength environments such as physiological conditions. One challenge regarding using HA/Ch PEMs in marine antifouling application is the stability of the coatings in such high salinity media. In a previous work HA/Ch PEMs were crosslinked using thermal crosslinking and chemical crosslinking in order to achieve stability in sea water and it was found that the marine antifouling performance critically depended on the method of crosslinking. Thermal crosslinking led to PEM coatings with good antifouling performance but yielded less hydrophilic surfaces with little protein resistance. Chemical crosslinked PEMs showed good protein resistance but were not reducing zoospore settlement (Yu et al. 2019). In other studies, cell adhesion was found to be enhanced on chemically crosslinked HA/Ch PEMs compared to as constructed PEMs (Richert, Boulmedais, et al. 2004; Richert, Engler, et al. 2004; Picart et al. 2005; Schneider et al. 2007), which was speculated to be caused by the increased stiffness and rigidity of the coatings after chemical crosslinking (Richert et al. 2004; Schneider et al. 2007). For marine applications, the reduced resistance due to crosslinking poses a problem as latter is essential in order to avoid degradation of the coatings.

Fish protect themselves against the attachment of unwanted species and against infections by the use of mucus layers rich in glycosaminoglycans, glycoproteins, and carboxylated and sulfated polysaccharides as a sacrificial top layer (Shephard 1994; Baum et al. 2003; Dash et al. 2018). Inspired by this, one antifouling strategy is to use non-toxic, degradable and erodible fouling-release coatings composed of hydrolysable polymers (Lejars et al. 2013) showing controlled ablation rates in order to enhance their fouling-release properties (Bressy et al. 2010; Lejars et al. 2013; Ma et al. 2013; Lejars et al. 2014; Xie et al. 2019; Gevaux et al. 2019). When in contact with seawater, such coatings can act as self-shedding coatings with sacrificial top layers that are removed along with attached living organisms that managed to stick to the fouling-release coatings and thus enhanced the performance of the paints. PEMs have been developed as degradable coatings using hydrolytically degradable polymers (Moskowitz et al. 2010) or using weak polyelectrolytes that lose their electrostatic attraction at extreme pH (Sukhishvili and Granick 2002; Yang and Rubner 2002; Wang et al. 2013) and in high salinity (Dubas and Schlenoff 2001; Schüler and Caruso 2001) environments. Such PEMs are well suited for applications such as controlled drug delivery (Schüler and Caruso 2001; Sukhishvili and Granick 2002; Moskowitz et al. 2010) and antibacterial coatings (Wang et al. 2013; Xu et al. 2018).

The concept of self-polishing, non-toxic coatings is increasingly being exploited for novel coating technologies and was successfully applied to layer-by-layer constructed polysaccharides based on dextranes and Ch showing good performance in particular against pathogenic bacteria. Despite their otherwise very promising properties, investigations about the marine antifouling activity of degradable HA/Ch multilayer coatings are currently lacking. This study intends to close this gap and synthesized PEM coatings based on HA/Ch and tailored their degradation rate for use in the marine environment. The PEMs were crosslinked thermally and

chemically under different conditions to produce either degrading coatings or highly stabilized ones. In order to analyze if the slow degradation and thus the formation of sacrificial overlayers is capable to support the antifouling activity of the coatings, they were tested regarding their protein resistance and marine antifouling performance against zoospores of the macroalga *U. linza* and the diatom *N. incerta*. The results showed that the slow degradation and thus the formation of sacrificial overlayers led to enhanced marine antifouling activity of the degradable HA/Ch PEMs compared to the highly stabilized ones, indicating both, the usefulness of the self-degrading concept, as also the general potential of polysaccharide based coatings with integrated self-polishing properties as effective approach for marine antifouling applications.

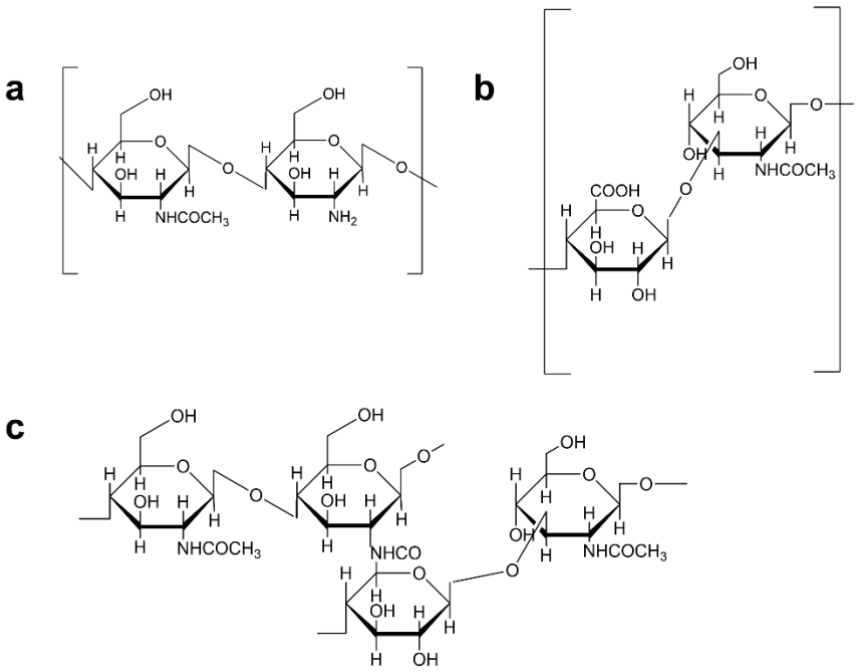

Figure 1. Molecular structure of the polysaccharides used to construct the PEMs: (a) Cationic chitosan (Ch), (b) anionic hyaluronic acid (HA) and (c) amide formation between Ch and HA.

Materials and Methods

Chemicals: 11-Amino-1-undecanethiol hydrochloride (AUDT), dodecanethiol (DDT), and α-undecyl-mercapto-ω-alkoxyl-hexa(ethylene glycol) (EG_6OH) were purchased from ProChimia Surfaces (Sopot Poland). Acetone (HPLC Grade) was obtained from Alfa Aesar (Ward Hill, MA, USA). All other chemicals were purchased from Sigma-Aldrich (St. Louis, MO, USA) and used without further purification. Deionized water was purified with a Milli-Q Plus system (Millipore, Schwalbach, Germany). Nexterion B clean room cleaned glass slides were purchased from Schott (Mainz, Germany). Phosphate buffered saline (PBS) buffer was obtained from Fisher Scientific (Pittsburgh, PA, USA) and used at pH 7.4.

Construction of polyelectrolyte multilayers (PEMs): PEMs were constructed on (3-aminopropyl)trimethoxy silane (APTMS)-functionalized silicon wafers or glass slides and for the SPR measurements on gold-coated AUDT functionalized SPR chips. APTMS functionalization of surfaces followed previously described protocols (Bauer et al. 2013). In

brief, the plasma activated surfaces were put in a sealed dry flask under N_2 atmosphere with 5% APTMS solution in dry acetone. The reaction was carried out for 30 min under ultra-sonication. The SPR chips were cleaned by sonication for 3 min in ethanol (p.a.) followed by immersion for 24 h in a 10 mM AUDT solution, which was followed by 3 min sonication in ethanol. Following previous literature reports, PEMs were constructed by spin coating. (Kelly and Schlenoff 2015) The construction of PEMs was carried out according to a previously published protocol (Yu et al. 2019). 1 mg/mL HA and Ch solutions at pH 4.5 with 0.15 M NaCl were used, Milli-Q water was used in the washing step. The multilayers were constructed using a spin coater WS-650MZ-23NPP/LITE from Laurell Technologies Corporation (North Wales, PA, USA). Substrates were initially spun at 1200 rpm for 10 s, then accelerated to 3000 rpm for 30 s. The procedure was repeated until the desired number of layer pairs of the $(HA/Ch)_i$ films (typically i = 7.5) were deposited. The multilayer construction started with HA and was terminated with HA.

Crosslinking of PEMs: PEMs were thermally crosslinked in a vacuum drying oven (Heraeus vacutherm, Thermo Electron Corporation, Waltham, MA, USA) for 6 h at 180 °C for high degree of crosslinking to produce stabilized coatings (denoted as TC180), and at 135 °C for 6 h for low degree of crosslinking (denoted as TC135). Chemical crosslinking was carried out through 1-ethyl-3-(3-dimethylaminopropyl)carbodiimide hydrochloride (EDC) and N-hydroxysuccinimide (NHS) chemistry. Therefore, a crosslinking solution containing 400 mM EDC and 100 mM NHS at pH 5.5 with 0.15 M NaCl was used in order to strongly chemically crosslink the PEMs (denoted as CC400). For the weakly crosslinked coatings, a solution with 250 µM EDC, but without any NHS, at pH 5.5 with 0.15 M NaCl was used (denoted as CC250). The surfaces were immersed into the EDC/NHS solution for 12 h, followed by three washing steps in 0.15 M NaCl solution for 1 h. After washing, surfaces were dried in a flow of dry nitrogen.

Preparation of reference monolayer coatings: Self-assembled monolayers (SAMs) were coated on gold substrates, which were cleaned under an ozone-generating UV lamp for 1 h followed by 3 min sonication in ethanol (p.a.) and then a thorough rinse with ethanol. The cleaned substrates were immersed into 1 mM dodecanethiol (DDT) or α-undecyl-mercapto-ω-alkoxyl-hexa(ethylene glycol) (EG_6OH) solutions for 24 h to allow the SAM to assemble. After 24 h, the substrates were again cleaned by sonication and rinsed with ethanol following the above described procedure.

Spectroscopic ellipsometry: PEM thicknesses were determined by spectroscopic ellipsometry with the device M-2000 from J. A. Woollam Co. Inc (Lincoln, NE, USA) at three incidence angles (65°, 70° and 75°) relative to the surface. The thickness of the coating was determined by modeling the obtained data as a transparent, single polymer layer with a wavelength-dependent refractive index described by the Cauchy model (A = 1.45, B = 0.01). There were three measurements on each sample and the average values are reported.

Water contact angle goniometry: Static water contact angle measurements were carried out with a custom-built goniometer. Droplets of tridistilled water were dispensed on the surface then recorded by a CCD camera. The water droplet shape was fitted by Young's equation to determine the contact angle. Three measurements were taken for each sample and the average values are reported.

Atomic force microscopy (AFM) measurement: The AFM images were measured with a NanoWizard® AFM from JPK Instruments AG (Berlin, Germany). A MULTI-75G (70 kHz) cantilever (BudgetSensors, Sofia, Bulgaria) was used in the tapping mode. Typical settings for a 10 µm × 10 µm scan were 1 V target amplitude, 0.5 V setpoint, 350 Hz igain, and 89 µm/s tip velocity. For measurements in liquids, the contact mode was used with a MULTI-75G cantilever. Typical settings were 0.3 V setpoint, 0.003 V p-gain and 200 Hz igain. The data was analyzed using Gwyddion (Version 2.47). Surface roughness was quantified as the RMS value calculated by the following equation:

$$R_{RMS} = \sqrt{\frac{1}{n}\sum_{i=1}^{n} |z_i^2|} \quad (1)$$

Where n is the number of data points and z_i is the height deviation of the i-th point from the average height. Three regions of interest with 100 × 100 pixels were analyzed and the average values are reported.

Fourier transform infrared spectroscopy in attenuated total internal reflection geometry (ATR-FTIR): PEMs were characterized by ATR-FTIR spectroscopy using a TENSOR 27 FTIR from Bruker (Billerica, MA, USA) equipped with a VariGATR^{TM} germanium ATR prism (Harrick Scientific Products, Inc, New York, USA), with a resolution of 4 cm^{-1}. Each measurement comprised 250 scans. The spectra were acquired with a liquid N_2 cooled mercury cadmium telluride (MCT) detector, in the wavenumber range of 4000-600 cm^{-1}.

Surface plasmon resonance (SPR) analysis: SPR measurements were carried out using a SR7000DC from Reichert Technologies Life Science (Munich, Germany). PEMs were built up on 12.5 mm × 12.5 mm glass slides. The slides were coated with a 50 Å titanium layer and a 600 Å gold layer on which a monolayer of aminoundecanethiol was assembled before the PEMs were constructed. Matching fluid of 1.515 refractive index (Cargille, Thermo Fisher Scientific, Waltham, MA, USA) was used to establish the optical contact between the prism of the SPR device and the SPR chip. Each SPR experiment started with PBS buffer flushing across the surface at a flow rate of 200 µL/min until a stable baseline was obtained. Subsequently, the PBS buffer flow rate was changed to 10 µL/min and the protein solution (1 mg/mL in PBS, pH 7.4) was injected into the system and incubated for 10 min. After the exposure phase, the surface was rinsed with PBS buffer to determine the irreversibly bound fraction of protein. The solutions of the proteins-fibrinogen, bovine serum albumin (BSA) and lysozyme (Sigma Aldrich, St. Louis, MO, USA)-were freshly prepared before each experiment. Each measurement was repeated three times, and the average values are reported.

PEM stability in aqueous media: PEM stability was investigated by immersing the multilayers for the desired time in Milli-Q water, PBS buffer (pH 7.4) or salt water (SW). To simulate the marine environment, SW that contained the major components (ion mass content > 50 ppm) of seawater (Kester et al. 1967) was used. As only synthetic salts were used, adsorption of macromolecules that might form conditioning layers (Thome et al. 2012) was avoided. The initial thickness and the one remaining after the different immersion steps were quantified by spectroscopic ellipsometry. Three measurements were taken on each sample, average thickness which was normalized to the initial thickness are reported.

***Ulva linza* zoospore settlement assay:** Mature plants of *U. linza* were collected at Craster, UK (55°26′ N; 1°35′ W) and spores were released and isolated by previously published methods (Callow et al. 1997). For the settlement assay, the multilayer-coated slides were immersed for 12 h in Milli-Q water, and then for 15 min in 0.22 µm-filtered artificial seawater (ASW) (Tropic Marin$^{@}$, Wartenberg, Germany) before analysis. A suspension of zoospores (10 mL; 1×10^6 spores·mL^{-1}) was added to individual compartments of quadriPERM$^{@}$ dishes (Sarstedt Inc, Nümbrecht, Germany) containing the samples. After incubation for 45 min, in darkness, at room temperature, the slides were washed by passing back and forth 10 times through a beaker of seawater to remove unsettled (i.e. swimming) spores. Slides were fixed using 2.5% glutaraldehyde in ASW. The density of zoospores attached to the surfaces was counted on each of the 3 replicate slides using Leica LAS-X image analysis system attached to a Zeiss Axioskop 2 fluorescence microscope. Spores were visualized by auto-fluorescence of chlorophyll. Counts were made for 30 fields of view (each 0.15 mm^2) on each slide. The number of settled spores was subjected to a one-way analysis of variance (ANOVA) with Tukey test for statistical significance analysis with a significance threshold of $p < 0.05$.

***Navicula incerta* removal assay:** Biological tests against the marine diatom *N. incerta* followed previously published protocols (Finlay et al. 2010). All slides were pre-immersed for 12 h in Milli-Q water and subsequently in 0.22 µm-filtered ASW for 15 min prior to the assay. *N. incerta* cells were cultured in F/2 medium and diluted to give a suspension with a chlorophyll *a* content of approximately 0.25 µg·mL^{-1}. Cells were allowed to settle on three replicate slides of each coating chemistry in individual quadriPERM$^{@}$ dishes (Sarstedt Inc, Nümbrecht, Germany) containing 10 mL of suspension at ~20 °C on the laboratory bench. After 2 h, the slides were exposed to 5 min of shaking on an orbital shaker (60 rpm) followed by immersion and washing in 0.22 µm-filtered ASW to remove cells which were not attached. Samples were fixed in 2.5% glutaraldehyde in ASW, air dried, and the density of cells attached to the surfaces was counted on each slide, using fluorescence microscopy. 30 fields of view (each 0.15 mm^2) were analyzed on each slide. Three more replicate slides of each coating chemistry were settled with cells of *N. incerta* as described above. Slides with attached cells were exposed to a shear stress of 27 Pa in a turbulent water channel (Schultz et al. 2000). Samples were fixed and the number of cells remaining attached was counted as described above. Data were analyzed by one-way ANOVA and post-hoc Tukey Test. The significance threshold was set at $p < 0.05$.

Results

Coating preparation and characterization

The major driving force for the HA/Ch layer-by-layer multilayer assembly is electrostatic attraction between the carboxylates from HA and the amines from Ch. The "as constructed" multilayer films are not stable in high salinity media, as ions strongly reduce the Debye length and thus reduce the electrostatic attraction between opposite charges. This can cause the disassembly of the multilayers. In order to covalently stabilize the multilayers, they can be thermally crosslinked (Muzzio et al. 2017) or chemically crosslinked with EDC/NHS chemistry (Picart et al. 2005). By controlling the crosslinking conditions (temperature, EDC/NHS concentration), strongly and weakly crosslinked multilayers were obtained. Reaction conditions in this study are summarized in Table 1, together with PEM labels and their properties (coating thickness, static water contact angle, and RMS roughness). PEMs without crosslinking were included as a reference.

PEM treatment	Label	Coating thickness (nm)	Static water contact angle (°)	RMS roughness (nm)
Not crosslinked	Non-crosslinked	57 ± 3	18 ± 3	1.9 ± 0.1
Thermally crosslinked at 135 °C	TC135	45 ± 1	63 ± 4	0.5 ± 0.1
Thermally crosslinked at 180 °C	TC180	35 ± 2	73 ± 4	2.0 ± 0.1
Chemically crosslinked using 250 µM EDC	CC250	54 ± 1	14 ± 2	2.2 ± 0.1
Chemically crosslinked using 400 mM/100 mM EDC/NHS	CC400	55 ± 2	20 ± 5	3.3 ± 0.1

Table 1. PEM properties characterized before and after crosslinking. In the list are labels of the coatings, dry coating thickness as determined by AFM (100 µm × 100 µm scan area) using a scratch in the polymer (average of 6 cross-sections, error bars are the standard deviation), static water contact angle (WCA) (average of three independent measurements are reported, error bars are the standard deviation), RMS roughness was measured with AFM in air across a 10 µm × 10 µm area. For RMS the average height deviation was calculated with equation 1, three region of interests were analyzed each with 100 × 100 pixels, average values are reported, errors are the standard deviation.

Properties of non-crosslinked and crosslinked PEMs are listed in Table 1. After both crosslinking processes, a decrease in thickness was observed. The chemical crosslinking method caused a slight thickness reduction: CC400 decreased by 3.5% and CC250 by 5.3% compared to the non-crosslinked PEMs. The thickness reduction in thermally crosslinked multilayers was found to be substantially higher and a decrease by 38.6% after crosslinking at 180 °C (TC180) and by 21.1% after crosslinking at 135 °C (TC135) was measured.

Water contact angle goniometry was used to characterize the wettability of the PEMs. The non-crosslinked PEM was hydrophilic with a WCA at 18 ± 3°. Chemically crosslinked PEMs showed similar hydrophilicity and CC400 had a WCA of 20 ± 5°, while that of CC250 was 14 ± 2°. After thermal crosslinking, the multilayers became more hydrophobic. TC180 and TC135 had WCAs of 73 ± 4° and 63 ± 4°, respectively.

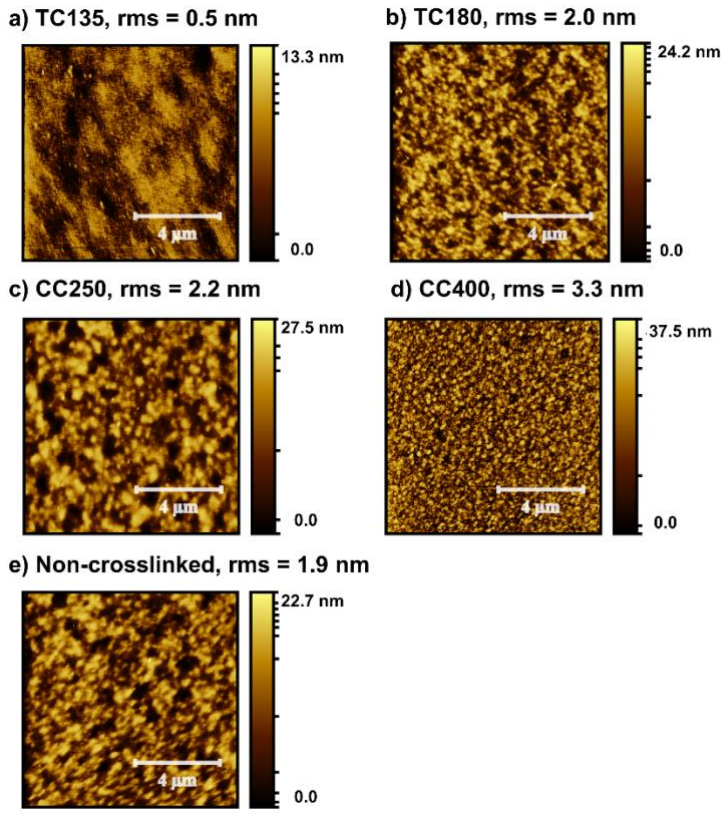

Figure 2. Surface morphology of the multilayer coatings measured by AFM: (a) TC135, (b) TC180, (c) CC250, (d) CC400 and (e) non-crosslinked. The width of each AFM image is 10 µm, RMS roughness is the average height deviation, calculated using equation 1 (values represent the average RMS values of 3 regions of interest each with 100 × 100 pixels).

Morphology of the PEMs was characterized using AFM (Figure 2). The native, non-crosslinked film had an RMS roughness of 1.9 ± 0.1 nm. TC135 had a lower RMS value of 0.5 ± 0.1 nm, whereas the RMS value for TC180 was 2.0 ± 0.1 nm. In the case of chemical crosslinking, a higher RMS value was observed, for CC250 at 2.2 ± 0.1 nm and for CC400 at 3.3 ± 0.1 nm. The different roughnesses also become apparent from the corresponding color bars for the height. The structures of the PEMs were also different and depended on the method of crosslinking. Features presented on TC180 (Figure. 2b) and CC250 (Figure. 2c) were still similar to the one on non-crosslinked PEMs (Figure. 2e), while CC400 showed a fine, granular, but very rough morphology (Figure. 2d). TC135 was rather smooth as reflected in its low RMS value and the low corrugation indicated by the height color bar (Figure. 2a).

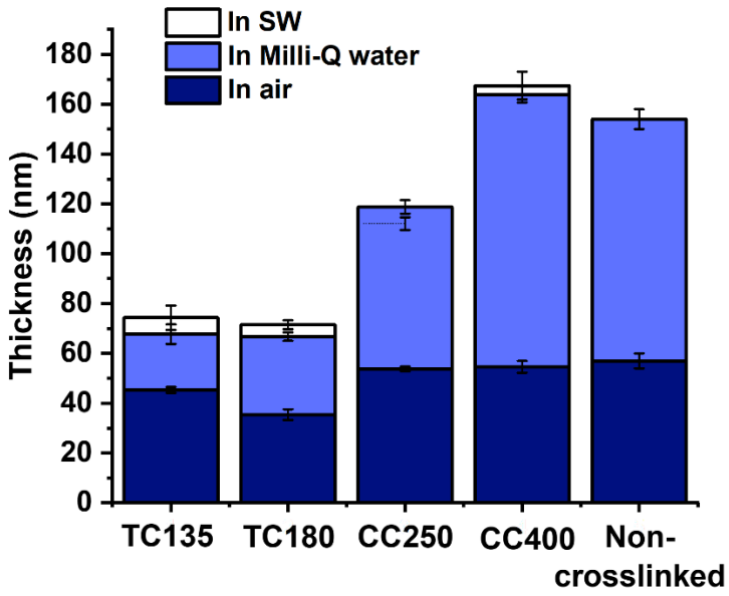

Figure 3. Thickness of PEM coatings determined by AFM using cross-sections of a scratch in the coatings. Thicknesses were measured in air (dark blue bars), in Milli-Q water (light blue bars), or in salt water SW (white bars) using scan areas of 100 × 100 µm. For each measurement, 6 cross-sections were acquired and average values along with the standard deviations (error bars) are reported. The dotted line on the CC250 bar indicates the coating thickness in SW which was slightly thinner than that in Milli-Q water.

Swelling behavior of the coatings was investigated by AFM. The thicknesses were determined in two media, Milli-Q water and SW. To determine the height of the coatings, a scratch was applied to expose the substrate and the thicknesses of cross-sections were measured by AFM. First, the thickness under dry conditions was measured, a subsequent measurement of the thickness in Milli-Q water or SW allowed the thickness of the hydrated coating to be determined (Figure 3). As already discussed, the dry PEMs possessed different thicknesses depending on the crosslinking protocol: Thickness of the non-crosslinked PEMs was 57 nm and of TC180 35 nm, TC135 45 nm, CC250 54 nm, and CC400 55 nm. When exposed to Milli-Q water, the thickness of the non-crosslinked PEMs increased to 154 nm, which is a thickness increase of 170%. Among the crosslinked PEMs, thermally crosslinked PEMs showed lower swelling tendency than the chemically crosslinked PEMs. TC135 and TC180 increased to 68 nm, which is a thickness increase of 51% and 94%, respectively. The thickness of the chemically crosslinked PEMs CC250 and CC400 increased from 54 nm to 118 nm and from 55 nm to 163 nm, which corresponds to an increase of 119% and 196%, respectively. When exposed to SW, the crosslinked PEMs retained their thickness even though the ion strength was strongly increased which created a different osmotic situation. Swelling of non-crosslinked PEMs in SW was not investigated due to the fast degradation of the coatings.

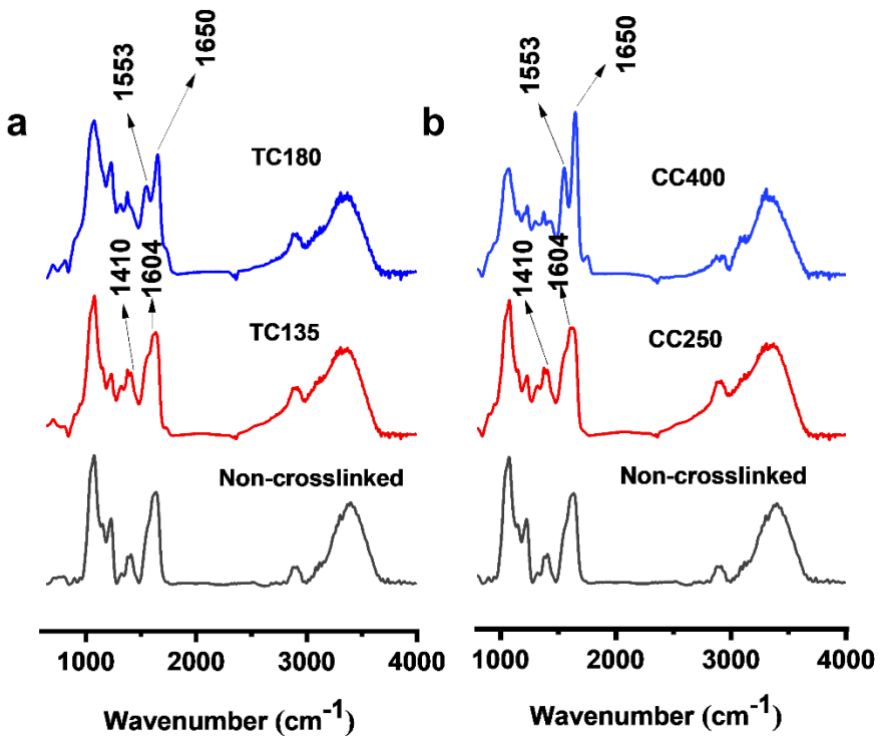

Figure 4. ATR-FTIR spectra of the PEMs: (a) TC135, TC180 and non-crosslinked PEMs. (b) CC250, CC400 and non-crosslilnked PEMs.

ATR-FTIR spectra of the crosslinked and the non-crosslinked pristine films are shown in Figure 4. The successful crosslinking is proven by the formation of amide groups between the carboxylates of HA and the amines of Ch. Figure. 4a shows the ATR-FTIR spectra of thermally crosslinked PEMs. Before crosslinking, PEM showed peaks originating from the carboxylates, at 1410 cm^{-1} and 1604 cm^{-1} (Richert, Boulmedais, et al. 2004). These two peaks remained in the spectrum of TC135, indicating that some carboxylates in TC135 still remained non-crosslinked. Crosslinking of TC135 was confirmed by the increased intensity of amide II peak at 1553 cm^{-1} (Almodovar et al. 2011). In the case of TC180, the carboxylate peaks were strongly reduced while the amide I and amide II peaks at 1650 cm^{-1} and 1553 cm^{-1} (Almodovar et al. 2011) increased substantially, indicating a higher degree of amide formation within the polyelectrolytes. Figure. 4b shows the ATR-FTIR spectra of chemically crosslinked PEMs. Similar to low-temperature thermal crosslinking, the CC250 spectrum was similar to that of the pristine film, with stronger peaks at 1410 cm^{-1} and 1604 cm^{-1}, and a slight increase in the amide peak intensity at 1553 cm^{-1} and 1650 cm^{-1}. This indicates free carboxylates remaining in the PEMs, and a weak crosslinking of the polyelectrolyte by amide formation. CC400 showed a higher intensity of the amide peaks at 1650 cm^{-1} and 1553 cm^{-1} while the carboxylate peaks were strongly reduced.

Stability and controlled degradation of the PEMs in different media

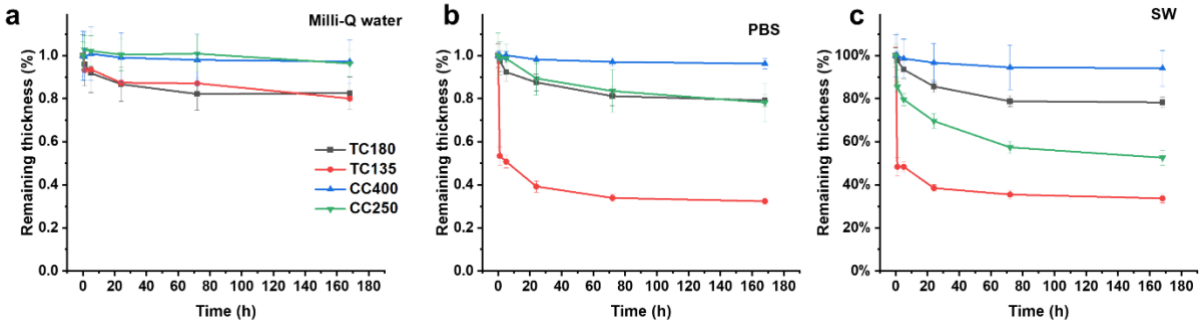

Figure 5. Stability and degradation of crosslinked HA/Ch multilayers in (a) Milli-Q water, (b) PBS and (c) SW. Three different media were used for the test: Milli-Q water, PBS buffer at pH 7.4, and SW on a linear shaking table. Average of three independent measurements on each sample are reported, error bars are the standard deviation.

To characterize the degradation behavior of the PEMs, the coatings were immersed in Milli-Q water, PBS buffer, or SW for a maximum of 7 days, on a linear shaking table at 55 rpm, and their thickness was monitored using spectroscopic ellipsometry (Figure 5). The stability of the PEMs in Milli-Q water is shown in Figure. 5a: After 7 days of immersion, less than 4% degradation was observed for the chemically crosslinked PEMs (CC250 96% remained, CC400 97% remained). In the case of thermal crosslinking, stability was slightly lower. After 7 days of immersion, 82% of TC180 and 80% of TC135 remained. Figure. 5b shows the stability of the coatings in PBS buffer as used for the protein resistance assays discussed below. CC400 was relatively stable in PBS, and after 7 days of immersion in PBS 96% of the coatings remained. During the same immersion period, CC250 was reduced to 78% of the initial coating thickness. The thickness of the thermally crosslinked PEM TC180 was reduced to 79% after 7 days of immersion; a comparable thickness reduction to that in Milli-Q water. TC135 showed a stronger degradation, after only 1 h immersion, the thickness decreased to 53% and after 7 days 32% of the coating thickness remained. Figure. 5c shows the stability of PEMs in SW. CC400 showed good stability and 94% of its thickness remained after 7 days of immersion. CC250 exhibited stronger degradation and after the first hour the thickness had already decreased to 85%, and after 7 days to 53%. The remaining thickness of TC180 after 7 days was 78%. TC135 showed a sharp initial drop of 48% after 1 h immersion, similar to that in PBS medium, and 34% remained after 7 days. While in Milli-Q water all coatings were stable, only the strongly crosslinked PEMs showed stability in SW. The partially crosslinked PEMs showed a continuous degradation over several days.

Antifouling tests

Protein adsorption on the PEM coatings

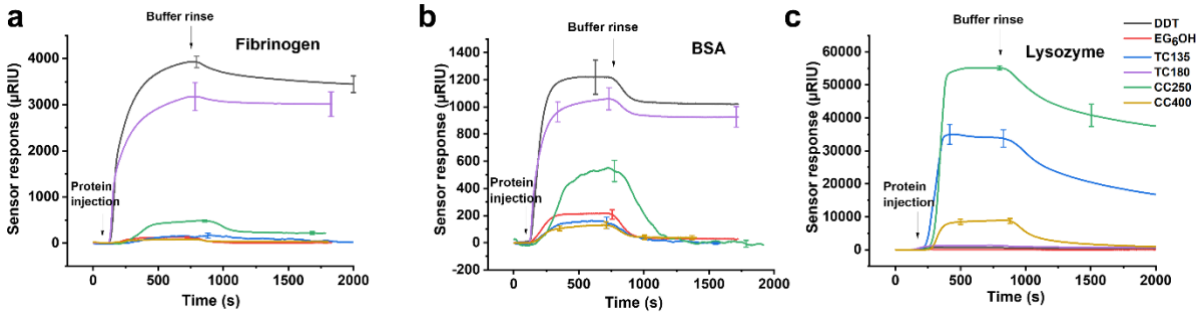

Figure 6. SPR sensorgrams of protein adsorption tests on PEMs against three proteins: (a) Fibrinogen, (b) BSA and (c) lysozyme. After a stabilized baseline was obtained during PBS buffer flow, protein solution was injected into the chamber for 10-min incubation followed by a rinsing phase with PBS buffer. Dodecanethiol (DDT)- and hexa(ethylene glycol) (EG_6OH)-terminated SAMs were included as negative and positive controls, respectively. Average of three independent measurements are reported, error bars are the standard deviation.

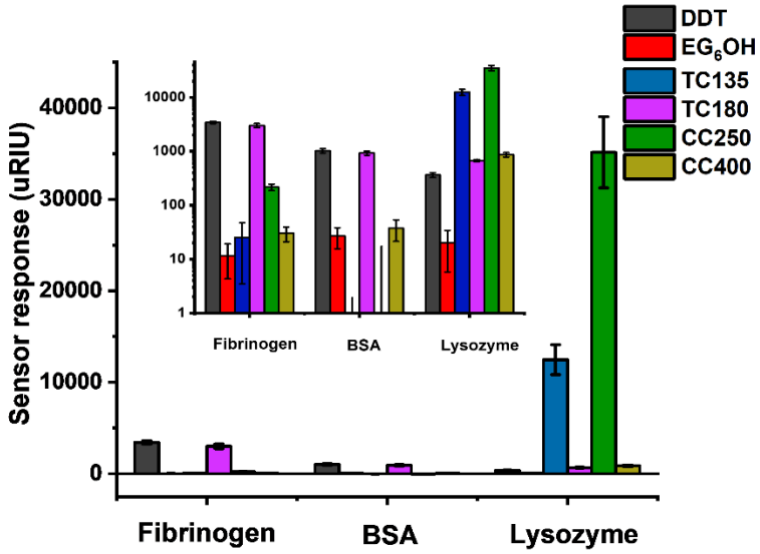

Figure 7. Non-specific protein adsorption on HA/Ch PEMs studied by SPR. Three proteins were tested, fibrinogen and BSA were negatively charged, lysozyme was positively charged at the pH of the buffer. Fibrinogen had a molecular mass of 340 kDa, BSA 69 kDa and lysozyme 14 kDa. Self-assembled monolayers consisting of dodecanethiol (DDT)- and of hexa(ethylene glycol) (EG_6OH)- terminated thiols were included as controls. The bargraphs show the amount of irreversibly attached proteins on PEMs and the control surfaces. The inset shows the results with a logarithmic y-scale to show trends for the very resistant surfaces. Reported values are the average of three measurements and error bars are the standard deviation.

The polyelectrolyte multilayers were first characterized towards their ability to resist non-specific protein adsorption. For this experiment, the PEM coatings were constructed on small glass chips with a thin gold layer and investigated by surface plasmon resonance spectroscopy (SPR). Both positively and negatively charged proteins were included in the adsorption assay. The multilayers were always terminated by HA. The SPR sensorgrams of fibrinogen, BSA and lysozyme on the PEMs are shown in Figure 6. DDT and EG_6OH were included in the assay as negative and positive controls, respectively. The amounts of protein remaining after rinsing with PBS (irreversibly adsorbed protein) is presented in Figure 7. TC135, CC250, and CC400 showed good resistance against non-specific adsorption of fibrinogen. Only TC180 accumulated the protein in amounts comparable to the hydrophobic DDT control. When tested against BSA, a similar trend was found and TC135, CC250, and CC400 all reduced non-specific adsorption to levels comparable to the EG_6OH control. Again, TC180 showed higher non-specific protein adsorption comparable to the DDT negative control. In the assay against the positively charged protein lysozyme, strong protein adsorption was observed, in particular on the weakly crosslinked PEMs TC135 and CC250. Only EG_6OH was able to effectively resist lysozyme adsorption.

Resistance of the PEM coatings against marine biofouling

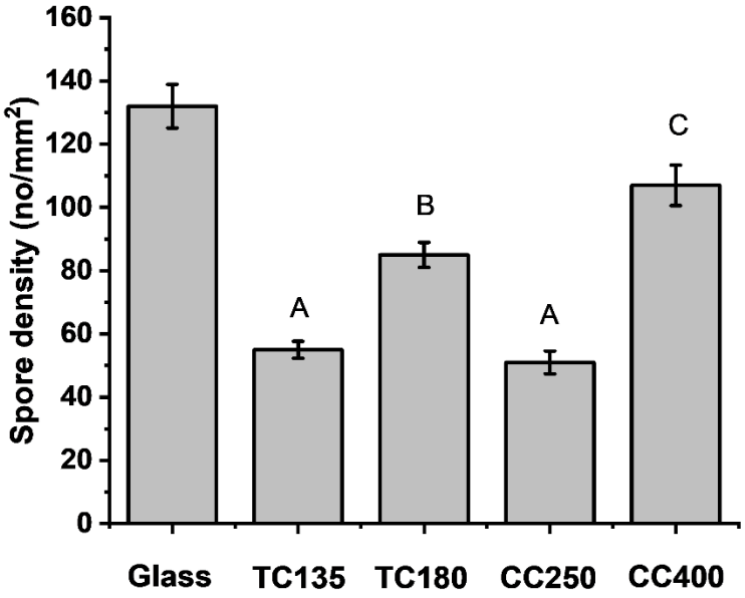

Figure 8. Density of zoospores of *U. linza* on the multilayer coatings after a 45-min settlement assay. Each value is the average of the settled spore densities in 90 fields of view on 3 replicate slides. Error bars are the standard error. Bars that do not share the same letter are statistically significantly different.

In order to test the antifouling properties of the PEM coatings, they were subjected to a settlement assay using zoospores of the macroalga *U. linza* (Callow et al. 2000). Figure 8 shows the densities of settled spores at the end of the 45-min assay. The lowest settlement was observed on the two partially crosslinked PEMs, TC135 and CC250. TC180 and CC400 attracted higher settlement. One-way analysis of variance found significant variation among the coatings. A post-hoc Tukey test showed that the settlement on CC400 was significantly higher than that on TC180, and both had significantly higher settlement than the partially crosslinked coatings, TC135 and CC250, which did not differ significantly (significant level of $\alpha = 0.05$).

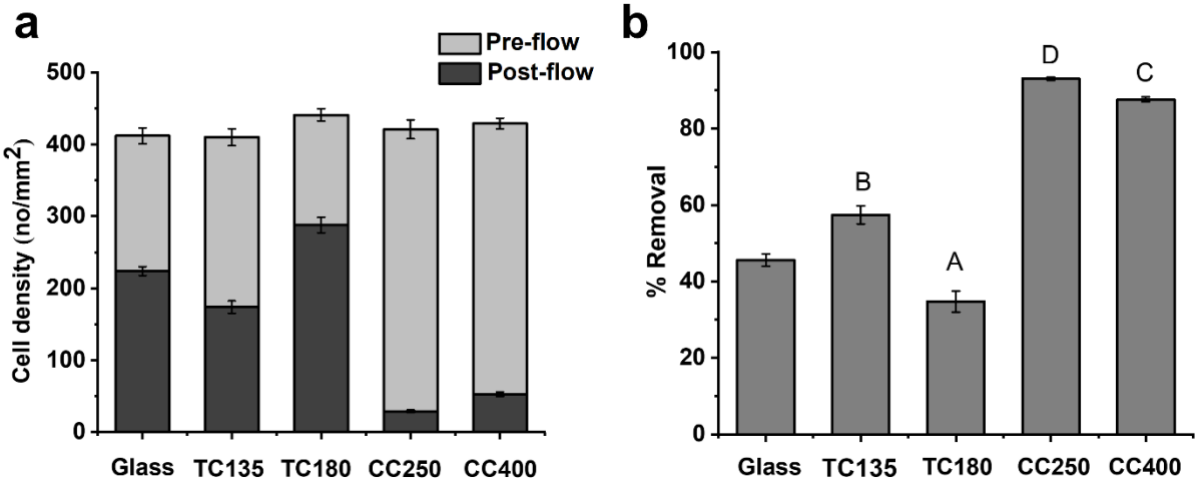

Figure 9. *N. incerta* attachment on the PEM coatings. (a) Density of *N. incerta* cells on the multilayer coatings before (gray) and after (black) exposure to a turbulent flow exerting a wall shear stress of 27 Pa. (b) Percentage of cells removed from the surface. Reported values are the average of the densities in 90 fields of view on 3 replicates slides. Error bars are the standard error. Bars that do not share the same letter are statistically significantly different.

The coatings were also tested against attachment and removal of the diatom *N. incerta* (Figure 9). Cells were allowed to settle on the surfaces for 2 h and subsequently exposed to a turbulent

water flow to remove unattached cells. The number of cells before ("Pre-flow") and after ("Post-flow") the application of the water flow was counted (Figure. 9a) and the percentage removal of cells was calculated (Figure. 9b). No statistically significant differences in initially attached cells ("Pre-flow") was observed on the HA/Ch coatings. Thus, the coatings do not actively hinder diatoms from making an attachment with the surface. After exposure to the turbulent flow, a substantial difference in cell densities between the four coatings was observed. From TC180 35% ± 5% were removed, while at a lower degree of crosslinking and thus a slow degradability of the coatings substantially increased the fouling-release properties as 57% ± 5% were removed from TC135. The chemically crosslinked PEMs showed even better performance and 88% ± 1% of the diatoms were removed from CC400. A weaker crosslinking and thus the introduction of a controlled degradability again led to a higher removal and 93% ± 1% of the diatoms were removed from CC250. A one-way ANOVA with post hoc Tukey test indicates that removal percentage on the four different coatings are statistically significantly different. (significance level of $\alpha = 0.05$).

Discussion

PEMs based on hyaluronic acid and chitosan were constructed by layer-by-layer assembly using spin coating. The multilayers obtained were crosslinked to different degrees resulting in either coatings that were stable or coatings with controlled degradation (self-polishing effect). The effects of thermal and chemical crosslinking methods on the properties of the PEMs were characterized in a number of ways. After thermal crosslinking, thickness of the PEMs decreased in the case of TC135 and TC180. This might be the result of a denser and more compact film structure, which would be in agreement with previous reports where HA/Ch PEMs were thermally annealed at 37 °C for 72 h which led to denser films according to the signal increase in circular dichroism (CD) (Muzzio et al. 2017). According to the AFM characterization, thermally crosslinked PEMs showed a rather smooth morphology in the dry state. This could be connected with the dense and strongly crosslinked structure, which was created by the simultaneous thermal crosslinking and drying process. With chemical crosslinking, a less dense polymer network might have been formed because crosslinking took place in an aqueous environment and the crosslinking might have locked the swollen and hydrated structures. Thus, in the dry state rougher structures were obtained. In both, thermal and chemical crosslinking, PEMs with a higher degree of crosslinking exhibited increased roughness. The general notion that crosslinking leads to rougher films is in good agreement with previous studies where dip-coated 6 µm thick HA/Ch films were crosslinked in a mixture of 400 mM EDC and 100 mM NHS solution. The crosslinked film had an increased RMS roughness of 39.6 nm compared to that of the non-crosslinked film at 7.3 nm (Schneider et al. 2007). The observed WCA changes due to crosslinking were in good agreement with a previous study in which thermal crosslinking generated hydrophobic surfaces whereas chemical crosslinking led to more hydrophilic coatings (Yu et al. 2019). Swelling of PEMs was investigated in two media, Milli-Q water and salt water. While in Milli-Q water the PEMs showed swelling ratios between 51% and 196%, which was influenced by the protocol used for crosslinking, it was observed that the swelling of the coatings in salt water resembled that in Milli-Q water, indicating that the swelling tendency of the PEMs was retained in high salinity medium.

The exposed charged groups after the PEMs came into contact with aqueous media can indirectly be deduced from the SPR protein resistance data. The good resistance against the negatively charged fibrinogen and BSA (in PBS pH 7.4) and the strong accumulation of the

positively charged lysozyme suggests that anionic groups dominate the surface of the PEMs, which is in favor for deterring *U. linza* zoospores settlement since the zeta potential of the motile spores is known to be -19.3 mV (Rosenhahn et al. 2009). Moreover, previous work found that non-crosslinked HA/Ch films were more prone to proteolytic degradation as pores were formed after exposure to lysozyme, amylase and natural saliva. Films crosslinked in a mixture of 400 mM EDC and 100 mM NHS in turn were more resistant to enzymatic degradation (Etienne et al. 2005). In particular, the observation that the weakly crosslinked PEMs in this work showed very high lysozyme adsorption could be connected to its inherent affinity to HA and Ch as potential substrates.

The thermally crosslinked degradable PEMs showed good resistance against nonspecific protein adsorption on the same level as the very hydrophilic chemically crosslinked PEMs. Since they were prepared at a lower temperature compared to TC180, TC135 had lower WCA of 63° while it was 73° in the case of TC180. According to the Berg limit, when a surface has WCA below 65°, the water structure near the surface becomes more compact and denser, which prevents protein adsorption on the surface (Berg et al. 1994; Erwin 1998). It could be that the difference in protein resistance of TC180 and TC135 reflects this transition of wettability through the Berg limit.

Fewer spores of *U. linza* settled on TC180 than on CC400, in agreement with a previous study (Yu et al. 2019) in which thermally highly crosslinked PEMs showed good resistance to *U. linza* while chemically crosslinked PEMs exhibited distinctly poor performance (Yu et al. 2019). This was surprising, as thermal crosslinking generated hydrophobic surfaces, which are in general more attractive to spores and chemically crosslinked PEMs were very hydrophilic (Schilp et al. 2007). It was speculated that the thermally crosslinked PEMs with contact angles around 70° had smoother surfaces, which could be advantageous for their antifouling properties. In the literature, chemical crosslinking with EDC/NHS chemistry led in several cases to lower resistance towards cell adhesion, e.g. for chondrosarcoma cells (Richert, Boulmedais, et al. 2004; Schneider et al. 2007), macrophages (Picart et al. 2005), and smooth muscle cells (Richert, Engler, et al. 2004). One possible reason for the decreased cell resistance after crosslinking was the increased film stiffness and rigidity (Schneider et al. 2007; Richert, Boulmedais, et al. 2004). When the multilayers were treated with low EDC concentrations, the obtained PEMs were less rough, more hydrophilic, and swelled more readily (119% for CC250 as compared to 51% for TC135). This together with its slowly degrading properties might be the reason why CC250 showed competent antifouling performance against the *U. linza* zoospores. The relevance of slow degradation and formation of a sacrificial layers is supported by the observation that thermal crosslinking at lower degree also resulted in better antifouling performance than for the highly crosslinked PEMs.

PEMs were also tested against attachment of the diatom *N. incerta*. Unlike zoospores of *U. linza* which can actively search and select surfaces that are suitable for settlement, diatoms have no exploration activity as they reach interfaces by gravity or water currents and can only move by gliding after settlement (Wetherbee et al. 1998). Our results showed that after incubating PEMs for 2 h in the diatom suspension followed by gentle washing, there was similar attachment on all PEMs. When attachment was challenged by the exposure to a turbulent flow, more diatoms were removed from degradable PEMs. The chemically crosslinked PEMs showed a better release performance than the thermally crosslinked PEMs. The different fouling-release performance of the chemically and thermally crosslinked multilayers against *N. incerta* diatoms could be due to the different hydrophilicity and/or hydration of the coatings. In a previous study,

despite a similar initial settlement density, more *N. incerta* diatoms were removed after exposure to a 53 Pa shear force from PEGylated and glass surfaces than from the more hydrophobic fluorinated polymers and from PDMS coatings (Krishnan et al. 2006). A similar result was obtained for dendritic polyglycerols. This highly hydrophilic coating was tested in a diatom removal assay with *N. incerta*. More than 92% of the diatoms were removed from the polyglycerol-coated surfaces whereas on the hydrophobic octadecylsilane (OTS) controls the removal was only 12% (Wanka et al. 2018). The swelling analysis by AFM revealed that chemically crosslinked PEMs have a higher affinity for water than thermally crosslinked PEMs, as a higher degree of swelling was observed (119% and 196% versus 51% and 94%). Also for diatoms, a higher removal from chemically crosslinked PEMs was measured than from thermally crosslinked PEMs. Similar to the results from the *U. linza* assay, the studies with diatoms showed that the degradable PEMs outperformed the non-degradable ones. This supported the initial idea that a slow degradation and the formation of a sacrificial surface layer of biopolymers would enhance the fouling-release properties of the coatings. It can be speculated that some of the diatoms were removed alongside part of the liberated polymer. This study has shown for the first time that the enhancement of fouling-release properties against marine biofouling organisms can be improved by introducing degradability into polyelectrolyte multilayer coatings constructed from aqueous solutions of natural occurring biomacromolecules. In so doing it supports the findings of previous publications that a certain degradability of coatings is favourable for the fouling-release efficiency (Gevaux et al. 2019).

Although thermal and chemical crosslinking methods yielded degradable coatings, the obtained PEMs possessed quite different properties. While thermal crosslinking produced hydrophobic, less hydrated, and smooth surfaces; chemical crosslinking led to hydrophilic, more hydrated, relatively rough coatings. Two marine species, zoospores of the macroalga *U. linza* and cells of the diatom *N. incerta* were removed more readily from the chemically crosslinked surfaces even though the fundamental chemistry was very similar in both systems. Hyaluronic acid and chitosan, two commonly used naturally occurring polymers with biocompatibility and biodegradability, have been used to prepare marine low-fouling coatings in several previous studies, as grafted monolayers (Cao et al. 2009; Bauer et al. 2013) or as mulitlayers (Xu et al. 2016; Xu et al. 2018; Yu et al. 2019). When HA and Ch are assembled into polysaccharide multilayers they face the particular challenge that they need to be stabilized by crosslinking when used in saltwater, which affects their antifouling performance (Yu et al. 2019). Using reduced crosslinking this effect was reduced and self-degrading properties led to enhanced antifouling performance of the coatings. The observed antifouling activity clearly highlights the versatility of the HA/Ch system. It also became obvious that a degradation, even if no active substances are released, is capable to reduce the attachment of marine organisms. Most likely this is due to the liberated macromolecules forming a sacrificial overlayer which is removed along with attached marine organisms. While this study was in first place designed as a conceptual study, further adjustment of properties such as the degradation rate might allow to use the degradable HA/Ch PEMs as an independent marine antifouling coatings for specific niche applications in the future. This study also reinforced the view that the material class of polysaccharides itself is worth being explored as hydrophilic compounds in amphiphilic acrylate or silicone antifouling coatings.

Conclusion

The naturally occurring biodegradable polysaccharides, hyaluronic acid and chitosan were constructed as degradable polyelectrolyte multilayers with marine fouling-release properties. The multilayers were deposited by spin coating and then crosslinked for enhanced stability. The degradability was attained by reducing the degree of crosslinking under mild reaction condition. While thermal crosslinking yielded a condensed and smooth coating with a lower tendency to hydrate and low hydrophilicity, with chemical crosslinking a rougher coating with enhanced hydrophilicity and stronger swelling behavior was produced. The multilayers showed superior protein resistance according to surface plasmon resonance spectroscopy and in particular the chemically crosslinked PEMs exhibited good fouling-release properties against two marine species, zoospores of the macroalga *U. linza* and the unicellular diatoms *N. incerta*. The introduction of a slow degradability reduced the problem that an enhanced stability in seawater requires crosslinking which in turn reduced the antifouling performance of HA/Ch PEMs. The formation of sacrificial layers that are removed along with the microbes could be a mechanism of the coatings. Fine tuning of the crosslinker system or the embedding of the polyelectrolytes into resins could be ways to exploit the interesting antifouling properties of the polysaccharide compounds investigated in this study.

* Corresponding Author:

Axel Rosenhahn:

axel.rosenhahn@rub.de

Acknowledgments

The work was funded by N00014-20-12244 (AR), ONR N00014-16-1-2988 (ASC), N00014-16-1-3125 (ASC and JAF). We acknowledge access to atomic force microscopy provided by Prof. W. Schuhmann, Analytical Chemistry- Electrochemistry, RUB.

Declaration of interest

The authors declared that they have no conflicts of interest to this work.

References

Arnon H, Granit R, Porat R, Poverenov E. 2015. Development of polysaccharides-based edible coatings for citrus fruits: A layer-by-layer approach. Food chemistry. 166: 465–472.

Almodóvar J, Place LW, Gogolski J, Erickson K, Kipper MJ. 2011. Layer-by-layer assembly of polysaccharide-based polyelectrolyte multilayers: A spectroscopic study of hydrophilicity, composition, and ion pairing. Biomacromolecules. 12: 2755–2765.

Al-Naamani L, Dobretsov S, Dutta J, Burgess JG. 2017. Chitosan-zinc oxide nanocomposite coatings for the prevention of marine biofouling. Chemosphere. 168: 408-417.

Arys X, Laschewsky A, Jonas AM. 2001. Ordered polyelectrolyte “multilayers”. 1. Mechanisms of growth and structure formation: a comparison with classical fuzzy “multilayers”. Macromolecules. 34: 3318–3330.

Bressy C, NGuyen MN, Tanguy B, van Ngo G, Margaillan A. 2010. Poly(trialkylsilyl methacrylate)s: A family of hydrolysable polymers with tuneable erosion profiles. Polym Degrad Stabil. 95: 1260–1268.

Baum C, Simon F, Meyer W, Fleischer LG, Siebers D, Kacza J, Seeger J. 2003. Surface properties of the skin of the pilot whale Globicephala melas. Biofouling. 19: 181–186.

Berg JM, Eriksson LGT, Claesson PM, Borve KGN. 1994. Three-component Langmuir-Blodgett films with a controllable degree of polarity. Langmuir. 10: 1225-1234.

Brady RF Jr, Singer IL. 2000. Mechanical factors favoring release from fouling release coatings. Biofouling. 15: 73–81.

Bauer S, Arpa-Sancet MP, Finlay JA, Callow ME, Callow JA, Rosenhahn A. 2013. Adhesion of marine fouling organisms on hydrophilic and amphiphilic polysaccharides. Langmuir. 29: 4039–4047.

Callow ME, Callow JA, Ista LK, Coleman SE, Nolasco AC, Lopez GP. 2000. Use of self-assembled monolayers of different wettabilities to study surface selection and primary adhesion processes of green algal (Enteromorpha) zoospores. Appl Environ Microb. 66: 3249–3254.

Callow ME, Callow JA, Pickett-Heaps JD, Wetherbee R. 1997. Primary adhesion of *Enteromorpha* (chlorophyta, ulvales) propagules: Quantitative settlement studies and video microscopy. J Phycol. 33: 938-947.

Croll TI, O'Connor AJ, Stevens GW, Cooper-White JJ. 2006. A blank slate? Layer-by-layer deposition of hyaluronic acid and chitosan onto various surfaces. Biomacromolecules. 7: 1610–1622.

Cao X, Pettit ME, Conlan SL, Wagner W, Ho AD, Clare AS, Callow JA, Callow ME, Grunze M, Rosenhahn A. 2009. Resistance of polysaccharide coatings to proteins, hematopoietic cells, and marine organisms. Biomacromolecules. 10: 907–915.

Cao X, Pettitt ME, Wode F, Arpa Sancet MP, Fu J, Ji J, Callow ME, Callow JA, Rosenhahn A, Grunze M. 2010. Interaction of zoospores of the green alga ulva with bioinspired micro- and nanostructured surfaces prepared by polyelectrolyte layer-by-layer self-assembly. Adv Funct Mater. 20: 1984–1993.

Decher G. 1997. Fuzzy nanoassemblies: toward layered polymeric multicomposites. Science. 277: 1232–1237.

Dhillon GS, Kaur S, Brar SK. 2014. Facile fabrication and characterization of chitosan-based zinc oxide nanoparticles and evaluation of their antimicrobial and antibiofilm activity. Int Nano Lett. 4: 107.

Del Hoyo-Gallego S, Pérez-Álvarez L, Gómez-Galván F, Lizundia E, Kuritka I, Sedlarik V, Laza JM, Vila-Vilela JL. 2016. Construction of antibacterial poly(ethylene terephthalate) films via layer by layer assembly of chitosan and hyaluronic acid. Carbohyd Polym. 143: 35–43.

Dash S, Das SK, Samal J, Thatoi HN. 2018. Epidermal mucus, a major determinant in fish health, a review. Iran J Vet Res. 19(2): 72-81.

Dubas ST, Schlenoff JB. 2001. Polyelectrolyte multilayers containing a weak polyacid: Construction and deconstruction. Macromolecules. 34: 3736–3740.

Efimenko K, Finlay J, Callow ME, Callow JA, Genzer J. 2009. Development and testing of hierarchically wrinkled coatings for marine antifouling. ACS Appl Mater Interfaces. 1: 1031–1040.

Etienne O, Schneider A, Taddei C, Richert L, Schaaf P, Voegel JC, Egles C, Picart C. 2005. Degradability of polysaccharides multilayer films in the oral environment: An in vitro and in vivo study. Biomacromolecules. 6: 726–733.

Elshaarawy RFA, Mustafa FHA, Geelen L, Abou-Taleb AEA, Tadros HRZ, Kalscheuer R, Janiak C. 2017. Mining marine shell wastes for polyelectrolyte chitosan anti-biofoulants: Fabrication of high-performance economic and ecofriendly anti-biofouling coatings. Carbohyd Polym. 172: 352–364.

Finlay JA, Bennett SM, Brewer LH, Sokolova A, Clay G, Gunari N, Meyer AE, Walker GC, Wendt DE, Callow ME, Callow JA, Detty MR. 2010. Barnacle settlement and the adhesion of protein and diatom microfouling to xerogel films with varying surface energy and water wettability. Biofouling. 26: 657-666.

Fujimoto T, Tsuchiya Y, Terao M, Nakamura K, Yamamoto M. 2006. Antibacterial effects of Chitosan solution® against Legionella pneumophila, Escherichia coli, and Staphylococcus aureus. Int J Food Microbiol. 112: 96–101.

Gevaux L, Lejars M, Margaillan A, Briand JF, Bunet R, Bressy C. 2019. Hydrolyzable additive-based silicone elastomers: A new approach for antifouling coatings. Polymers**.** 11: 305.

Hu Z, Finlay JA, Chen L, Betts DE, Hillmyer MA, Callow ME, Callow JA, DeSimone JM. 2009. Photochemically cross-linked perfluoropolyether-based elastomers: Synthesis, physical characterization, and biofouling evaluation. Macromolecules. 42: 6999–7007.

Jakobi V, Schwarze J, Finlay JA, Nolte KA, Spöllmann S, Becker HW, Clare AS, Rosenhahn A. 2018. Amphiphilic alginates for marine antifouling applications. Biomacromolecules. 19: 402–408.

Kester DR, Duedall IW, Connors DN, Pytkowicz RM. 1967. Preparation of artificial seawater. Limnol Oceanogr. 12: 176-179.

Keskin DS, Tezcaner A, Korkusuz P, Korkusuz F, Hasirci V. 2005. Collagen–chondroitin sulfate-based PLLA–SAIB-coated rhBMP-2 delivery system for bone repair. Biomaterials. 26: 4023–4034.

Kelly KD, Schlenoff JB. 2015. Spin-coated polyelectrolyte coacervate films. ACS Appl Mater Interfaces. 7: 13980–13986.

Kong M, Chen XG, Xing K, Park HJ. 2010. Antimicrobial properties of chitosan and mode of action: a state of the art review. Int J Food Microbiol. 144: 51–63.

Kujawa P, Moraille P, Sanchez J, Badia A, Winnik FM. 2005. Effect of molecular weight on the exponential growth and morphology of hyaluronan/chitosan multilayers: A surface plasmon resonance spectroscopy and atomic force microscopy investigation. J Am Chem Soc. 127: 9224–9234.Kim S, Gim T, Kang SM. 2015. Versatile, tannic acid-mediated surface PEGylation for marine antifouling applications. ACS Appl Mater Interfaces. 7: 6412–6416.

Krishnan S, Wang N, Ober CK, Finlay JA, Callow ME, Callow JA, Hexemer A, Sohn KE, Kramer EJ, Fischer DA. 2006. Comparison of the fouling release properties of hydrophobic fluorinated and hydrophilic PEGylated block copolymer surfaces: Attachment strength of the diatom Navicula and the green alga Ulva. Biomacromolecules. 7: 1449–1462.

Kumar S, Ye F, Dobretsov S, Dutta J. 2019. Chitosan nanocomposite coatings for food, paints and water treatment applications. Appl Sci. 9 (12): 2409.

Leonardi AK, Ober CK. 2019. Polymer-based marine antifouling and fouling release surfaces: Strategies for synthesis and modification. Annu Rev Chem Biomol. 10: 241–264.

Lichter JA, van Vliet KJ, Rubner MF. 2009. Design of antibacterial surfaces and interfaces: polyelectrolyte multilayers as a multifunctional platform. Macromolecules. 42: 8573–8586.

Lejars M, Margaillan A, Bressy C. 2012. Fouling release coatings: A nontoxic alternative to biocidal antifouling coatings. Chem Rev. 112: 4347–4390.

Lejars M, Margaillan A, Bressy C. 2013. Well-defined graft copolymers of tert-butyldimethylsilyl methacrylate and poly(dimethylsiloxane) macromonomers synthesized by RAFT polymerization. Polym. Chem. 4: 3282-3292.

Lejars M, Margaillan A, Bressy C. 2014. Synthesis and characterization of diblock and statistical copolymers based on hydrolyzable siloxy silylester methacrylate monomers. Polym. Chem. 5: 2109-2117.

Liu X, Huang R, Su R, Qi W, Wang L, He Z. 2014. Grafting hyaluronic acid onto gold surface to achieve low protein fouling in surface plasmon resonance biosensors. ACS Appl Mater Interfaces. 6: 13034–13042.

Ma C, Xu L, Xu W, Zhang G. 2013. Degradable polyurethane for marine anti-biofouling. J. Mater. Chem. B. 1: 3099-3106.

Moskowitz JS, Blaisse MR, Samuel RE, Hsu HP, Harris MB, Martin SD, Lee JC, Spector M, Hammond PT. 2010. The effectiveness of the controlled release of gentamicin from polyelectrolyte multilayers in the treatment of Staphylococcus aureus infection in a rabbit bone model. Biomaterials. 31: 6019–6030.

Morra M, Cassineli C. 1999. Non-fouling properties of polysaccharide-coated surfaces. J Biomater Sci Polym Ed. 10: 1107–1124.

Muzzio NE, Pasquale MA, Diamanti E, Gregurec D, Moro MM, Azzaroni O, Moya SE. 2017. Enhanced antiadhesive properties of chitosan/hyaluronic acid polyelectrolyte multilayers driven by thermal annealing: Low adherence for mammalian cells and selective decrease in adhesion for Gram-positive bacteria. Mat Sci Eng C-Mater. 80: 677–687.

Picart C, Schneider A, Etienne O, Mutterer J, Schaaf P, Egles C, Jessel N, Voegel JC. 2005. Controlled degradability of polysaccharide multilayer films In vitro and In vivo. Adv. Funct. Mater. 15: 1771–1780.

Petrone L, Di Fino A, Aldred N, Sukkaew P, Ederth T, Clare AS, Liedberg B. 2011. Effects of surface charge and Gibbs surface energy on the settlement behaviour of barnacle cyprids (Balanus amphitrite). Biofouling. 27: 1043–1055.

Pitt WG, Morris RN, Mason ML, Hall MW, Luo Y, Prestwich GD. 2004. Attachment of hyaluronan to metallic surfaces. J Biomed Mater Res A. 68: 95–106.

Rosenhahn A, Ederth T, Pettitt ME. 2008. Advanced nanostructures for the control of biofouling: The FP6 EU Integrated Project AMBIO. Biointerphases. 3: IR1-5.

Rosenhahn A, Finlay JA, Pettit ME, Ward A, Wirges W, Gerhard R, Callow ME, Grunze M, Callow JA. 2009. Zeta potential of motile spores of the green alga Ulva linza and the influence of electrostatic interactions on spore settlement and adhesion strength. Biointerphases. 4: 7–11.

Rosenhahn A, Sendra GH. 2012. Surface sensing and settlement strategies of marine biofouling organisms. Biointerphases. 7: 63-76.

Richert L, Boulmedais F, Lavalle P, Mutterer J, Ferreux E, Decher G, Schaaf P, Voegel JC, Picart C. 2004. Improvement of stability and cell adhesion properties of polyelectrolyte multilayer films by chemical cross-linking. Biomacromolecules. 5: 284–294.

Richert L, Engler AJ, Discher DE, Picart C. 2004. Elasticity of native and cross-linked polyelectrolyte multilayer films. Biomacromolecules. 5: 1908–1916.

Richert L, Lavalle P, Payan E, Shu XZ, Prestwich GD, Stoltz JF, Schaaf P, Voegel JC, Picart C. 2004. Layer by layer buildup of polysaccharide films: Physical chemistry and cellular adhesion aspects. Langmuir. 20: 448–458.

Schneider A, Richert L, Francius G, Voegel JC, Picart C. 2007. Elasticity, biodegradability and cell adhesive properties of chitosan/hyaluronan multilayer films. Biomed Mater. 2: 45-51.

Schüler C, Caruso F. 2001. Decomposable hollow biopolymer-based capsules. Biomacromolecules. 2: 921–926.

Shephard KL. 1994. Functions for fish mucus. Rev Fish Biol Fisher. 4: 401–429.

Schultz MP, Bendick JA, Holm ER, Hertel WM. 2011. Economic impact of biofouling on a naval surface ship. Biofouling. 27: 87–98.

Schultz MP, Finlay JA, Callow ME, Callow JA. 2000. A turbulent channel flow apparatus for the determination of the adhesion strength of microfouling organisms. Biofouling. 15: 243–251.

Sanpui P, Murugadoss A, Prasad PD, Ghosh SS, Chattopadhyay A. 2008. The antibacterial properties of a novel chitosan–Ag-nanoparticle composite. Int J Food Microbiol. 124: 142–146.

Sukhishvili SA, Granick S. 2002. Layered, erasable polymer multilayers formed by hydrogen-bonded sequential self-assembly. Macromolecules. 35: 301–310.

Schilp S, Kueller A, Rosenhahn A, Grunze M, Pettitt ME, Callow ME, Callow JA. 2007. Settlement and adhesion of algal cells to hexa(ethylene glycol)-containing self-assembled monolayers with systematically changed wetting properties. Biointerphases. 2: 143–150.

Tsai GJ, Su WH. 1999. Antibacterial activity of shrimp chitosan against Escherichia coli. J Food Protect. 62: 239–243.

Thome I, Pettitt ME, Callow ME, Callow JA, Grunze M, Rosenhahn A. 2012. Conditioning of surfaces by macromolecules and its implication for the settlement of zoospores of the green alga Ulva linza. Biofouling. 28: 501–510.

Townsin RL. 2003. The ship hull fouling penalty. Biofouling. 19: 9–15.

Vogler EA. 1998. Structure and reactivity of water at biomaterial surfaces. Adv Colloid Interface Sci. 74: 69–117.

Wang BL, Ren KF, Chang H, Wang JL, Ji J. 2013. Construction of degradable multilayer films for enhanced antibacterial properties. ACS Appl Mater Interfaces. 5: 4136–4143.

Wanka R, Finlay JA, Nolte KA, Koc J, Jakobi V, Anderson C, Clare AS, Gardner H, Hunsucker KZ, Swain GW. 2018. Fouling-release properties of dendritic polyglycerols against marine diatoms. ACS Appl Mater Interfaces. 10: 34965–34973.

Wetherbee R, Lind JL, Burke J, Quatrano RS. 1998. Minireview—the first kiss: Establishment and control of initial adhesion by raphid diatoms. J Phycol. 34: 9–15.

Xu G, Liu P, Pranantyo D, Neoh KG, Kang ET. 2018. Dextran-and chitosan-based antifouling, antimicrobial adhesion, and self-polishing multilayer coatings from pH-responsive linkages-enabled layer-by-layer assembly. ACS Sustain Chem Eng. 6: 3916–3926.

Xu G, Pranantyo D, Xu L, Neoh KG, Kang ET, Teo SLM. 2016. Antifouling, antimicrobial, and antibiocorrosion multilayer coatings assembled by layer-by-layer deposition involving host–guest interaction. Ind. Eng. Chem. Res. 55: 10906–10915.

Xing K, Chen XG, Liu CS, Cha DS, Park HJ. 2009. Oleoyl-chitosan nanoparticles inhibits Escherichia coli and Staphylococcus aureus by damaging the cell membrane and putative binding to extracellular or intracellular targets. Int J Food Microbiol. 132: 127–133.

Xie Q, Pan J, Ma C, Zhang G. 2019. Dynamic surface antifouling: mechanism and systems. Soft Matter. 15: 1087–1107.

Yang SY, Rubner MF. 2002. Micropatterning of polymer thin films with pH-sensitive and cross-linkable hydrogen-bonded polyelectrolyte multilayers. J Am Chem Soc. 124: 2100–2101.

Yu W, Koc J, Finlay JA, Clarke JL, Clare AS, Rosenhahn A. 2019. Layer-by-layer constructed hyaluronic acid/chitosan multilayers as antifouling and fouling-release coatings. Biointerphases. 14: 51002-51012.

Zhou J, Romero G, Rojas E, Ma L, Moya S, Gao C. 2010. Layer by layer chitosan/alginate coatings on poly (lactide-co-glycolide) nanoparticles for antifouling protection and Folic acid binding to achieve selective cell targeting. J Colloid Interface Sci. 345: 241–247.

Zhu X, Jańczewski D, Guo S, Lee SSC, Parra Velandia FJ, Teo SLM, He T, Puniredd SR, Vancso GJ. 2015. Polyion multilayers with precise surface charge control for antifouling. ACS Appl Mater Interfaces. 7: 852–861.

Zhu X, Jańczewski D, Lee SSC, Teo SLM, Vancso GJ. 2013. Cross-linked polyelectrolyte multilayers for marine antifouling applications. ACS Appl Mater Interfaces. 5: 5961–5968.